Preparation and Properties of Eu^{3+} Complex/ Polyimide Nano-composites

Li-juan Bian, Zi-kang Zhu*, Hong-jie Xu, Xue-feng Qian, Xiao-dong Ma, Jie Yin
(School of Chemistry and Chemical Technology, Shanghai Jiao Tong University, Shanghai 200240, China)

The property improvement of polymers via the homogenous incorporation of metallic salts and organometallic complexes within a polymer matrix is being actively pursued [1-4]. Various metallic salts and organo-metallic complexes have been synthesized and many polymers used as the matrix. Polyimides are a type of high-performance polymer widely applied in various industries because of their outstanding chemical resistance, mechanical properties, electrical properties, and radiation resistance, especially at elevated temperature. Recently, polyimide containing inorganic nano-particles has attracted a lot of attention [5-9]. Among the inorganic materials, Rare earth has been widely studied due its optical properties and complex ability and some of the hybrid of rare earth with common polymer has been prepared. However, the reports on the polyimide containing rare earth ions are limited. Southward et al. have worked on the hybrid system of fluorinated polyimide doped by lanthanide ions [5, 9-11]. The results showed that the incorporation of lanthanide complexes could effectively lower the coefficient of thermal expansion (CTE). In this study, we prepared europium (III)/polyimide hybrids and has studied some of the properties.

The composites were prepared from Eu^{3+} complex with poly (amic acid) solution which was based on two conventional monomers: benzophenone-3,3',4,4'-tetracarboxylic dianhydride (BTDA) and 4,4'-Oxydianiline (ODA) . The rare earth complex — EuL_3 (L= pyridine carboxylic acid) was prepared from Eu_2O_3, pyridine carboxylic acid and NaOH according to the reference[12].

The X-ray diffraction patterns of the virgin and doped polyimide films are shown in Fig. 1. Only one broad peak associated with the matrix polyimide was observed in both samples. Meanwhile, no crystalline calorimetric exotherms were found in their DSC curves (Fig. 5). Both results indicated that EuL3 existed in the amorphous state in the polyimide film.

Fig. 2 shows the TEM photograph of PI/EuL3-3 film, which reveals that EuL3 dispersed homogeneously in the hybrid with a particle size of about 20nm. This good dispersion of EuL_3 in PI was clearly caused by the strong interaction between them, which limited the aggregation of EuL3.

Fig 3 shows the mechanical properties of the composite films. The introduction of a very small amount of EuL3 leads to a clear increase in the tensile strength. Compared to the virgin PI, the introduction of 1 wt% EuL_3 leads to an increase of 23% in tensile strength. This increase was probably caused by the strong interaction between EuL_3 and PI, which makes EuL_3 act as a crosslink point. Since EuL3 was well dispersed in PI, only a small amount of EuL_3 led to a large amount of the cross-linking points. However, further increase in the EuL3 content caused a decrease in the tensile strength, probably due to the more amounts of the rare earth complex leads to the more potential of EuL3 to form aggregates. The hybrid containing 3 wt% EuL3

had similar tensile strength to the virgin PI.

The introduction of EuL3 also led to a linear increase in the Young's modulus of the hybrid (Fig. 4). The introduction of only 3 wt% EuL3 led to a 73% increase in the Young's modulus on the basis of the virgin PI (from 1.4Gpa to 2.4 Gpa). This dramatic increase in the modulus was caused by the strong interaction between the EuL3 and the PI, which limited the segmental movement of PI.

The strong interaction between EuL3 and PI would also lead to an increase in the glass transition temperature of the composites, which was confirmed by their DSC curves (Fig. 5 and Table 1). It showed that the Tgs modest increased with the increased of the EuL3 content. Since the glass transition process is related to the molecular motion [13], the strong interaction between EuL3 and PI can limits the cooperative motions of the polyimide main chain segments.

Meanwhile, their TGA curves (Fig. 6) also revealed that the thermal stability of the hybrids was also improved with the addition of EuL3. The temperatures at 10wt% are shown in table 1. When the EuL3 content is only 3wt%, the 10wt% decomposition temperature was enhanced 16°C. This may be due to the strong interaction between EuL3 and PI. The significance is that increasing the thermal stability of the polymer films by the incorporation of only small amount of rare earth complex. Moreover, the kinetic of increasing the thermal stability of the PI/EuL_3 is duo to the strong coordinate characteristic of Eu^{3+}, and this characteristic can also adapt to other rare earth elements.

The thermal expansion coefficient (CTE) is an important parameter to indicate the thermal mismatch for protective coating applications. Polyimide usually possesses a relatively low thermal expansion coefficient compared to other polymer duo to their rigid structure. PI/ EuL_3 composites have a potential to be a relatively low CTE materials because the strong interaction between EuL3 and PI. We studied the thermal expansion behavior of the PI/ EuL3 composites with a temperature range 75-125°C, see table 1. The CTE of the hybrids decreased with increasing the content of EuL3. The CTE decrease was 16.4 % for a very low EuL3 content (<3%). Due to the fine dispersion of EuL3 and strong interaction between EuL3 and PI, the expansion of polyimide chains were obstructs.

Since atoms of a rare earth element are large and have great polaribility, rare earth element containing materials usually have a high refractive index. From Fig. 7 we also found that the introduction of EuL_3 increased the refractive index of polyimide. When the EuL_3 content was 10wt%, the refractive index of the hybrid was 1.7889 at 633nm, much higher than that of the virgin PI (1.7086). The increase in the refractive index by the addition of EuL3 may have potential application in optical and electronic devices.

In conclusion, EuL3/PI hybrids have been successfully prepared. EuL3 was very well dispersed in the PI matrix due to the strong interaction between EuL3 and PI. The hybrids possess improved tensile strength and Young's modulus, increased glass transition temperature, thermal stability, size stability and refractive index compared to PI.

References

1. H. M. Zeng, Z. Y. Zhang and S. L. Wu, Polymer, 35, 1092, (1994).
2. M. W. Ellison, L. T. Taylor, Chem. Mater., 6, 990, (1994).
3. T. Sawada and S. Ando, Chem. Mater., 10, 3368, (1998).
4. R. V. Kumar, Y. Diamant, and A. Gedanken, Chem. Mater., 12, 2301, (2000).
5. R. E. Southward, D. S. Thompson, T. A. Thornton, D. W. Thompson and A. K. St. Clair, Chem. Mater., 10, 486, (1998).
6. L. Troger, H. Hunnefeld, S. Nunes, M. Oehring, D. Fritsch, J. Phys. Chem., B, 101, 1279, (1997).
7. D. Fritsch, K. V. Peinemann, Catal. Today, 25, 277, (1995).
8. D. Fritsch, K. V. Peinemann, J. Membr. Sci., 99, 29, (1995).
9. M. Nandi, J. A. Conklin, L. Jr. Salvati, A. Sen, Chem. Mater., 2, 772, (1990).
10. R. E. Southward, D. S. Thompson, D. W. Thompson and A. K. St. Clair, J. Adv. Mater., 27, 2, (1996).
11. D. S. Thompson, R. E. Southward, A. K. St. Clair, Polym. Mater. Sci. Eng., 71, 725, (1994).
12. R. E. Southward, D. S. Thompson, D. W. Thompson, T. A. Thornton, A. K. St. Clair, Polym. Mater. Sci. Eng., 76, 185, (1997).
13. T. Agag, T. Koga, T. Takeichi, Polymer, 42, 3399, (2001).

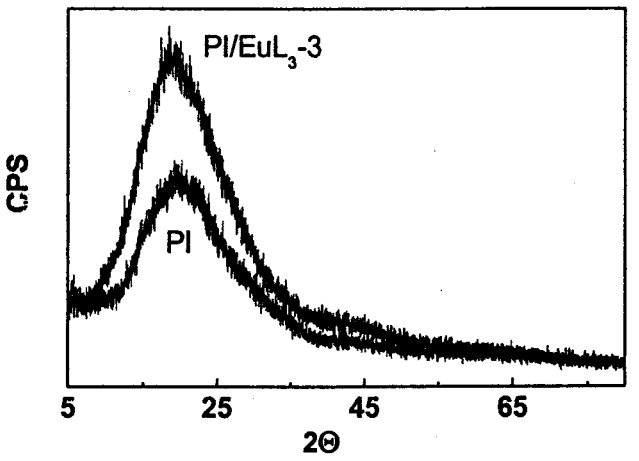

Fig. 1 X-ray diffraction patterns of PI / EuL_3 -3 and virgin PI

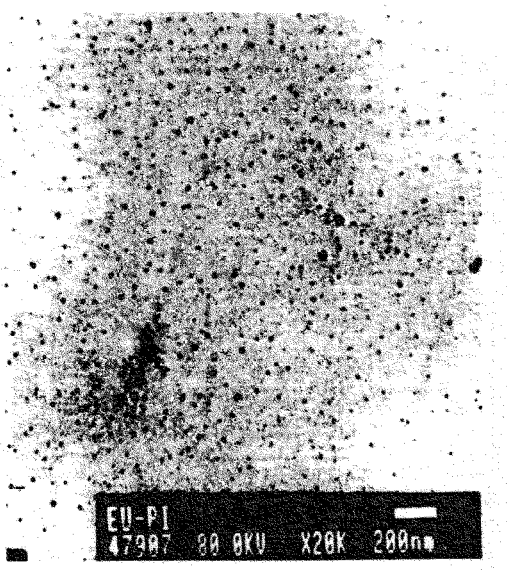

Fig.2 TEM photograph of PI / EuL_3-3

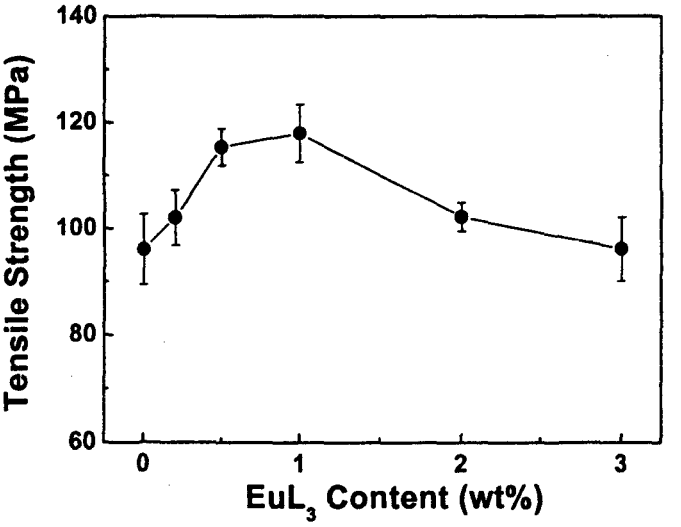

Fig 3 Mechanical properties of PI/ EuL_3 composite films

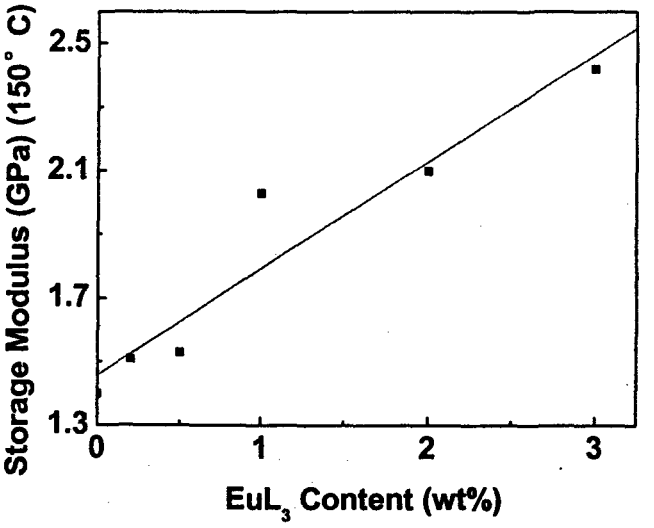

Fig 4 Relationship between the EuL_3 content and Young's modulus of PI /EuL_3 composite films

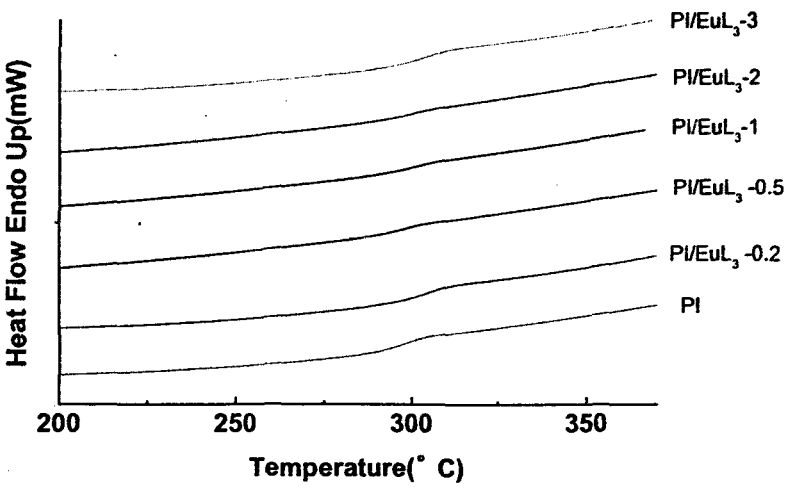

Fig. 5 DSC curves of PI and PI/EuL_3composites

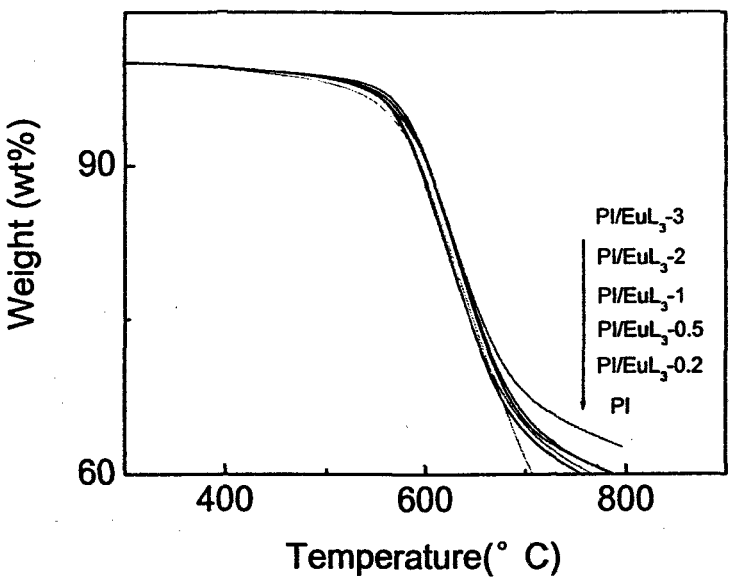

Fig. 6 TGA curves of PI and PI/EuL_3 composites

Table 1 Thermal properties of PI/EuL_3 hybrids

	PI	PI/EuL_3-0.2	PI/EuL_3-0.5	PI/EuL_3-1	PI/EuL_3-2	PI/EuL_3-3
Tg (°C)[a]	298.3	299.4	302.3	304.1	307.0	317.9
T_{10} (°C)[b]	563.2	569.9	571.4	573.7	576.7	579.7
CTE (10^{-6}/K)[c]	45.6	40.8	40.6	39.5	39.0	38.1

a: Glass transition temperature measured with DSC under the protection of N_2 with a scan rate of 20°C/min.

b: Temperature at 10% weight loss measured by TGA under the protection of N_2 with a scan rate of 20°C/min.

c: Coefficient of linear thermal expansion measured with DMA with TMA mode.

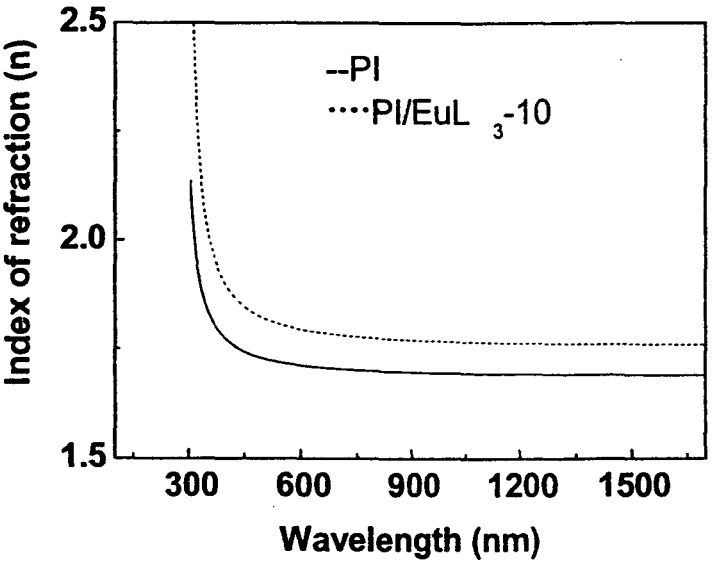

Fig. 9 Index of refraction of PI and